

Production, bonding strength and electrochemical behaviour of commercially pure Ti/Al₂O₃ brazed joints

O. C. PAIVA*, M. A. BARBOSA‡

*INEB-Instituto de Engenharia Biomédica, Praça do Coronel Pacheco 1, 4050 Porto, *also ISEP-Polytechnic Engineering Institute of Porto, Dept. of Mechanical Engineering, Rua de S. Tomé, 4200 Porto, and ‡ also Dept. of Metallurgical Engineering, FEUP, Rua dos Bragas, 4099 Porto Codex, Portugal*

The brazing of commercially pure titanium to Al₂O₃ has been studied. Two different brazing alloys within the Ag–Cu–Ti system and pure silver were selected as bonding agents. Titanium hydride (TiH₂) additions were also tested, with the aim of improving the wetting of the ceramic surface by the melted brazing alloy. The mechanical and electrochemical behaviour of the produced joints was assessed, and related to chemical and morphological features resulting from an analysis by scanning electron microscopy and energy dispersive spectroscopy. It was possible to produce joints presenting high integrity, good strength and high resistance to corrosion. The best results were obtained when using an Ag–26Cu–3Ti brazing alloy. The addition of TiH₂ increased the mechanical properties, leading to a maximum bonding strength of 80 ± 8 MPa, as determined in three-point bending tests. In most of the cases, for a maximum deflection of 5 mm, there was only a partial detachment of the ceramic/metal joints. The lowest values for the corrosion rates ($i_{\text{corr}} = 1.38 \mu\text{A cm}^{-2}$) determined in potentiodynamic experiments also correspond to the use of the Ag–26Cu–3Ti brazing alloy. The bonding strength and electrochemical results could be explained in terms of the different chemical compositions of the interfaces. The use of TiH₂ additions proved to be quite effective, allowing for the replacement of the usual metallizing and plating pre-treatments needed for the brazing of ceramics to metals.

1. Introduction

The unique properties of structural ceramics, such as alumina, make them well suited for a range of applications. This type of material is becoming increasingly important in engineering, especially in both structural and insulating applications [1, 2]. However, ceramics present poor machinability and their brittle nature limits a more extensive use. In order to avoid the processing limitations, some form of joining is usually employed to form the final component. The joint may be of either a ceramic/ceramic or a ceramic/metal type. Brazing is the most effective and widely used technique for joining structural ceramics (such as alumina) to ceramics and to metals [3–6].

The joining techniques currently used require metallization of the ceramic [3]. The ceramic is initially metallized by applying a Mn–Mo paste which is then burned in. To improve brazing properties, a nickel coating is then applied on top. The brazing process can then be carried out with conventional brazing alloys. While the process is complex, it can be considerably simplified by using active brazing alloys, without separate pretreatment [3, 4].

For a successful braze, the ceramics must be wetted by metals and alloys to produce strong bonds. However, many technologically important ceramics are unwetted by conventional brazes based on copper and silver [3, 4, 7]. To achieve the necessary wetting, the chemistry of the metal/ceramic interface must be changed and hence some components of the braze must be active enough to alter the composition and the chemistry of the ceramic surface [3, 7–9]. It is now well established that the wetting properties of various metals and alloys can be dramatically improved by small additions of titanium, aluminium, silicon and other interfacially active elements [3, 4, 7]. An active element may be defined as one which can interact with the ceramic and form a strong chemical bond at the interface [6, 10]. The improvements in the wetting behaviour produced by titanium additions are very frequently accompanied by improvements in the strength of brazed joints [7].

Bonding of materials, such as ceramics and metals, with distinct thermal expansion coefficients can be a problem, especially when heat is applied [8]. In addition, thermal shock, loss of hermetic sealing

and increase in the corrosion susceptibility at the metal/ceramic interface are areas for concern [11].

2. Experimental procedure

2.1. Materials

Metal/ceramic (M/C) joints were produced by an active metal brazing technique. Commercially pure titanium (Ti c.p.), grade 2, and alumina (Al_2O_3) 99.6% purity, prepared according to DIN 40685 standard, were selected to produce the joints. To produce these joints, Ti c.p. sheets with dimensions 30 mm \times 10 mm \times 0.8 mm and Al_2O_3 discs with a diameter of 8 mm and a thickness of 1.5 mm, were used. Two different brazing alloys within the Cu–Ag–Ti system and pure silver were selected as bonding agents. The composition of the alloys was as follows (wt %): Ag–26 Cu–3 Ti (alloy L1) and Ag–46 Cu–6 Ti (alloy L2). In both brazing alloys, discs with a diameter of 8 mm and a thickness of 0.3 mm were utilized.

2.2. Sample preparation

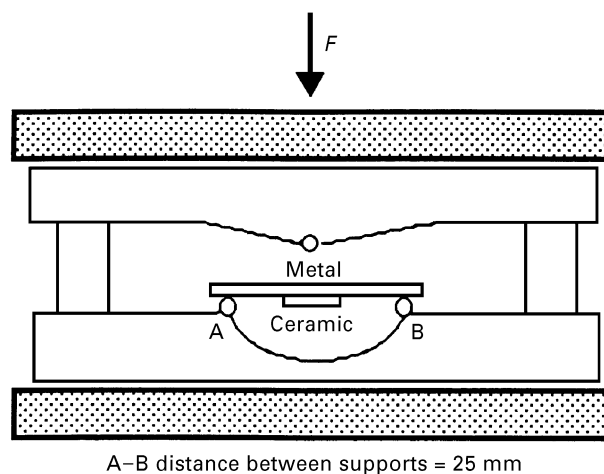
Before joining, the surfaces to be brazed were polished mechanically and then carefully surface cleaned by degreasing with acetone and rinsing with distilled water. Titanium hydride (TiH_2) additions were also tested, with the aim of improving the wetting of the ceramic surface by the molten brazing alloy. A TiH_2 dispersion was made using ethylene glycol as solvent (with a ratio of 1 g TiH_2 to 1 cm^3 solvent). Then the dispersion was spreaded on to the ceramic surface to be joined to the metal.

It was found that the brazing temperature of alloy L1 should be 850 °C, while alloy L2 should work at 950 °C and silver at 1000 °C. In all cases, the optimized holding time was 20 min. The heating and cooling rates used must be as slow as possible. Optimized values were 5 °C min^{-1} for heating and 1.2 °C min^{-1} for cooling. All joints were produced using a high-vacuum system. The vacuum level was typically in the order of 10^{-2} Pa (during the holding time).

2.3. Bonding strength measurements

In order to measure the bond strength of a metal/ceramic joint, a three-point bending loading scheme was selected. The samples were tested at a deformation rate 1 mm min^{-1} , in a universal Shimadzu mechanical testing machine. The experimental apparatus was as represented in Fig. 1.

Both the charging system and the sample dimensions were in accordance with ASTM/DE-855-84 Standard. The forces applied were not intended to lead the metal to fracture. Instead, they corresponded either to a maximum deflection of 5 mm, to “decohesion” at the interface, or to total fracture of the ceramic. Bonding strength was calculated using the three-point bending expression. It was assumed that the force needed to induce ceramic detachment was a good measurement of the interfacial bond strength.



A–B distance between supports = 25 mm

Figure 1 Schematic drawing of the three-point bending experimental apparatus used for the bonding strength determinations.

2.4. Electrochemical characterization

Electrochemical characterization of brazing alloys and Ti c.p./ Al_2O_3 bondings, was carried out using open-circuit and potentiodynamic experiments. In both cases, pure isotonic saline solutions (0.15 M NaCl solution) at room temperature (20 ± 2 °C) were used as testing environments. All the potentials were measured against a saturated calomel electrode (SCE) Tacussel XR100 and the electrochemical cell dimensions were in accordance to ASTM G5-82 Standard.

In open-circuit experiments, the specimens were immersed in the solution and their corrosion potentials were monitored for at least 60 min via a potentiostat/galvanostat (EGI G PAR, model 273) using adequate electrochemical software (SOFTCORR[®]). The potentiodynamic experiments were carried out with a potentiostat/galvanostat (EGI G PAR, model 273). The polarization started at -900 mV and ended at 1600 mV for all the specimens. The potential scanning rate was 5 mV s^{-1} .

The level of metal ions (titanium, copper and silver) released to the testing solutions, after the d.c. corrosion experiments carried out in the Ti/ Al_2O_3 bondings, were determined by atomic absorption spectroscopy (AAS). The measurements were carried out in a Instrumentation Laboratory IL 357 equipment.

2.5. Morphology and microcomposition of the M/C interfaces

The microstructures before and after electrochemical characterization, and the fractured surface of the joints after being submitted to the three-point bending testing were observed and analysed by scanning electron microscopy (SEM) in a Jeol JSM-35C and energy dispersive spectroscopy (EDS) in Noran instruments equipment.

3. Results and discussion

3.1. SEM/EDS characterization of Ti c.p./Ag/ Al_2O_3 bondings

Ti c.p. was bonded together with Al_2O_3 using pure silver as brazing agent. In order to produce proper

joints, TiH_2 has to be used in all cases as an intermediate layer between the ceramic and the silver disc. These kinds of interfaces were aimed to be used as control in the electrochemical tests (because both brazing alloys L1 and L2 contain silver in their chemical composition). A good penetration of TiH_2 in the Al_2O_3 superficial porosity was observed. Also, no cracks, resulting from the thermal cycle, were observed at the interface. Diffusion of titanium across the silver layer in the direction of the ceramic was not detected. Titanium, if present, could be deriving both from Ti c.p. and the TiH_2 layer. Nevertheless, the presence of microporosity near the ceramic surface was observed. On the other hand, at the Ti c.p./Ag interface, porosity or micro-cracks, which could be generated due to the different thermal expansion coefficient of the two metals, were not detected.

3.2. SEM/EDS characterization of Ti c.p./L1/ Al_2O_3 bondings

The best Ti c.p./ Al_2O_3 bondings, in terms of integrity and continuity, were achieved with brazing alloy L1, using the TiH_2 wetting layer. Fig. 2 presents a general view of the bonding. Figs. 3 and 4 are higher magnifications of the interfaces Al_2O_3 /L1 and L1/Ti c.p., respectively.

In Fig. 3, two adjacent layers, resulting from TiH_2 addition, may be observed. A central region, presenting a dendritic microstructure rich in silver and copper (white areas) surrounded by a matrix composed basically of copper and titanium (dark areas), may be seen. As we approach the L1/Ti c.p. interface (Fig. 4), dendrites tend to become larger and the region becomes richer in a mixture of titanium and copper. The interface itself is difficult to distinguish due to the quite slow attenuation of the overall chemical composition. The diffusion phenomenon plays a key role in the interface morphology. A needle-like phase seems to penetrate the titanium surface.

EDS results, reported in Table I, indicate that the amount of titanium within the brazing alloy region has increased with respect to its original composition. It appears that this titanium originates mainly from the metal. The EDS data indicate that there was a migration of titanium from the interface with Al_2O_3 (resulting from TiH_2 additions) to the brazing alloy region. Titanium seems to react with copper to form an intermetallic compound, Cu_xTi , with a composition very similar to the needle-like phase, basically composed of titanium and copper. In this case, titanium originates from the Ti c.p. substrate. The value of x is approximately 1.1 for region A (of Figs. 2 and 3) and 1.2 for the needle-like region as determined by EDS.

The above result is in accordance with Cassidy *et al.*'s. [12] observations. These authors have also identified, in Ti/ Al_2O_3 bondings produced using brazing alloys containing titanium, an intermetallic compound at the Al_2O_3 / brazing alloy interface. Its composition was Cu_xTi with x ranging from 1.2–1.6. This compound was a result of a reaction between the copper of the brazing alloy and titanium diffusion to

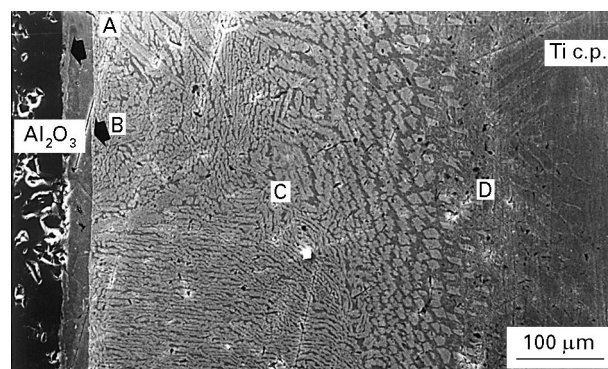


Figure 2 Scanning electron micrograph of the Al_2O_3 /L1/Ti c.p. joint, with TiH_2 addition. It is possible to notice several distinct morphologies, between the Al_2O_3 and the titanium, corresponding to quite different chemical compositions. ($\times 300$).

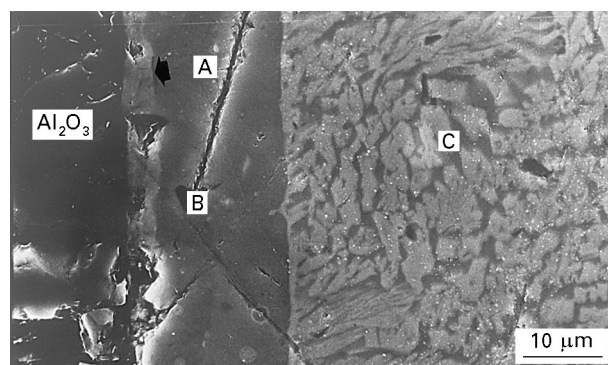


Figure 3 Magnification of the Al_2O_3 /L1 interface presented in Fig. 2. No gaps or cracks may be observed. ($\times 1500$).

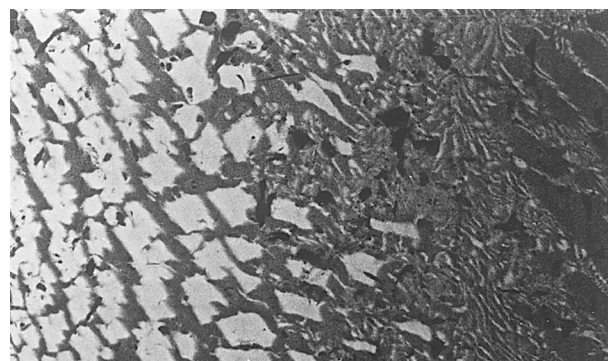


Figure 4 Magnification of the L1/Ti c.p. interface presented in Fig. 2. A needle-like structure may be observed. ($\times 1000$).

TABLE I Chemical composition of the Al_2O_3 /L1/Ti interface, determined by EDS

Layer designation	Layer thickness (μm)	Layer composition (at %)			
		Ag	Cu	Ti	Al
A	3–4	13.4	38.2	34.1	14.3
B	16–18	38.9	31.4	29.0	0.7
C	–	40.1	26.6	32.3	1.1
D	–	4.4	52.4	43.2	–

the Al_2O_3 interface. On the other hand, the layer identified as A (Figs. 2 and 3) has aluminium in its composition. Barbier *et al.* [13] reported, in $\text{Al}_2\text{O}_3/\text{Ti}-6\text{Al}-4\text{V}$ bondings, an oxide with a rather complex composition near the $\text{Al}_2\text{O}_3/\text{Cu}-40\text{Ag}-5\text{Ti}$ interface. They claim that this $\text{Cu}_2(\text{Ti}, \text{Al})_4\text{O}$ compound was responsible for the very good bonding obtained [13].

Loehman and Tomsia [14] reported that titanium reacts with Al_2O_3 to give a reaction layer containing oxygen and titanium in a ratio of 0.4–0.6 that is consistent with the information of $\text{TiO}_{0.5}$ and Ti_3Al .

These explanations seem to have one identical source. The titanium of the brazing alloy is segregated to the adjacent area of Al_2O_3 . This is due to its affinity with oxygen, as Al_2O_3 is the principal available source of this element (notice that the bonding process was carried out in a high vacuum). When titanium is being segregated, it will combine with copper forming an intermetallic compound. Also, the release and dissolution of oxygen and aluminium from the Al_2O_3 into the molten brazing alloy may occur, originating very complex reactions [15–18]. Under these conditions, it is possible that complex oxides similar to those identified by Barbier *et al.* [13] may be formed.

3.3. SEM/EDS characterization of Ti c.p./L2/ Al_2O_3 bondings

Ti c.p./ Al_2O_3 joints, without any addition of TiH_2 as an intermediate layer, could also be produced using the brazing alloy L2 at a holding temperature of 950°C . Fig. 5a and b represent, respectively, scanning electron micrographs of an L2/ Al_2O_3 interface and an L2/Ti c.p. interface. In Fig. 5a, a good bonding between the brazing alloy and the alumina may be observed. The dark points observed near that interface were identified by EDS as being titanium. However, the titanium concentration detected near the L2/Ti c.p. interface (Fig. 5b) is higher than the average alloy L2 composition. That anomaly in the concentration of the titanium from the brazing alloy near to the Ti c.p./L2 interface is, presumably, the result of the higher tendency of titanium (from the brazing alloy) to diffuse into the metallic Ti c.p.

We must also stress that the titanium present in the chemical composition of alloy L2 (6% weight) may be considered as one of the major causes of the good adhesion obtained between the L2 brazing alloy and Al_2O_3 . In fact, titanium additions to the brazing alloys affect their interfacial chemical interaction with ceramic oxides [12]. On the other brazing alloy, elements proved to be distributed almost randomly along the bonding.

3.4. Mechanical characterization of Ti c.p./ Al_2O_3 bondings

As far as the M/C bonding strength characterization is concerned, three types of behaviour were observed (in all cases after the application of a maximum deflection of 5 mm). These types of behaviour may be classified as follows.

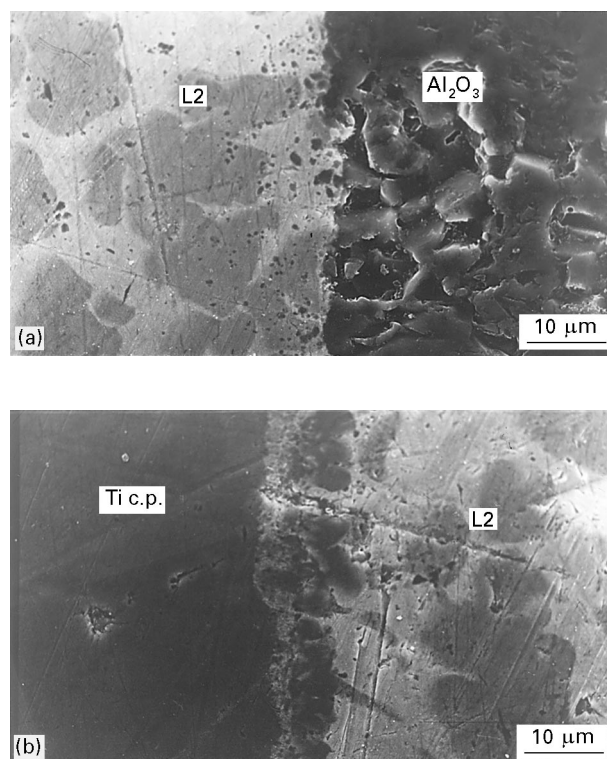


Figure 5 Scanning electron micrographs of (a) the $\text{Al}_2\text{O}_3/\text{L2}$ interface, and (b) the Ti c.p./L2 interface. ($\times 1000$).

(A) The fracture evolution occurs through the alumina, parallel to the $\text{Al}_2\text{O}_3/\text{brazing alloy}$ interface, but no total fracture of the joint was observed.

(B) Total decohesion, fracture nucleation and its propagation occurred across the alumina.

(C) The fracture nucleation occurred within the alumina and the fracture propagation through it, with fracture zones within the brazing alloy leading to the total fracture of the joint.

Fig. 6 illustrates the Ti c.p./L1/ Al_2O_3 joint, with a TiH_2 intermediate layer, after a three-point bending test. Even after reaching a 5 mm deflection there was no metal/ceramic detachment (fracture of type A). This was the most common situation with TiH_2 additions. It was observed by SEM that cracks propagate intergranularly in the alumina close to the brazing alloy. Cassidy *et al.* [12] have proposed a model to explain the fracture mode of alumina ceramics brazed with a Cu–Ag alloy using a titanium intermediate layer. The fracture propagation is located along the alumina and not directly in the interface.

In samples brazed with alloy L1, without TiH_2 additions, and tested for bonding strength, the observation of the fractures by SEM indicates that crack propagation occurs along the alumina (Type B) or in a more irregular way within the region of the brazing alloy (Type C).

Fig. 7 represents the interface Ti c.p./L2 after the three-point bending test and Fig. 8 the corresponding EDS spectrum of the fracture surface. In Fig. 7 it is clear that the fracture occurred preferentially through the Al_2O_3 . However, some detachments of the brazing alloy were also observed. This information may be complemented by the analysis of the EDS spectrum in Fig. 8 in which an attempt was made to acquire the

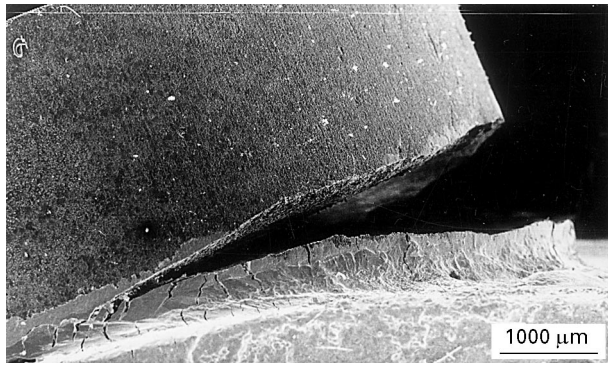


Figure 6 One aspect of the Ti c.p./L1/Al₂O₃ joint, with TiH₂ addition, after a typical three-point bending test. No total detachment of the ceramic from the metal could be observed even after applying a 5 mm deflection. ($\times 30$).

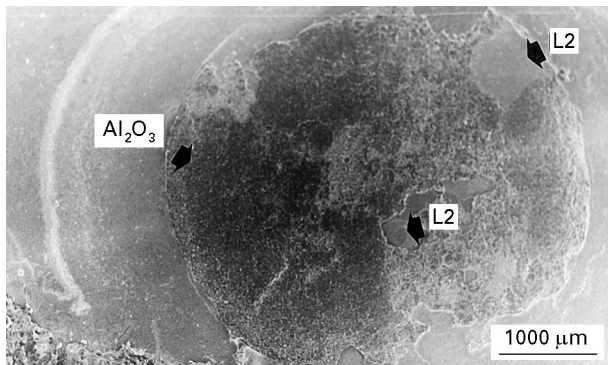


Figure 7 The Ti c.p./L2 fracture surface after a three-point bending test. ($\times 10$).

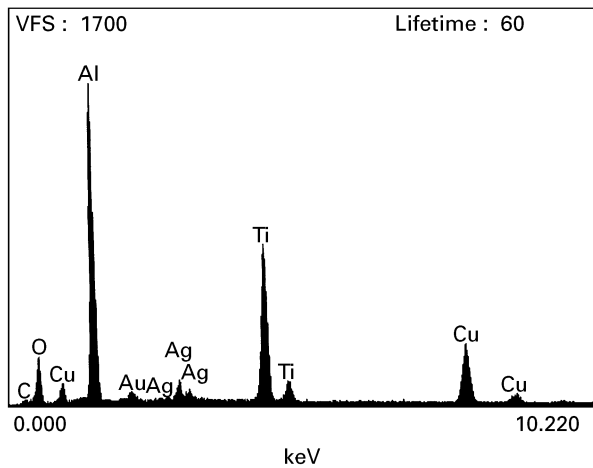


Figure 8 EDS spectrum of a fracture surface of the Ti c.p./L2 interface. The fracture was propagated preferentially along the alumina but indicated small penetrations in the brazing alloy.

signal from the whole fracture zone shown in Fig. 7. In this spectrum it is possible to detect a very strong aluminium peak corresponding to the Al₂O₃ zones bonded to the Ti c.p./L2 interface. The high intensity of the titanium peak may be justified, in part, by the impossibility of eliminating the interaction with the nearby metallic substrate when acquiring the EDS spectra.

Fig. 9 presents the results obtained in the three-point bending tests. The best results were attained

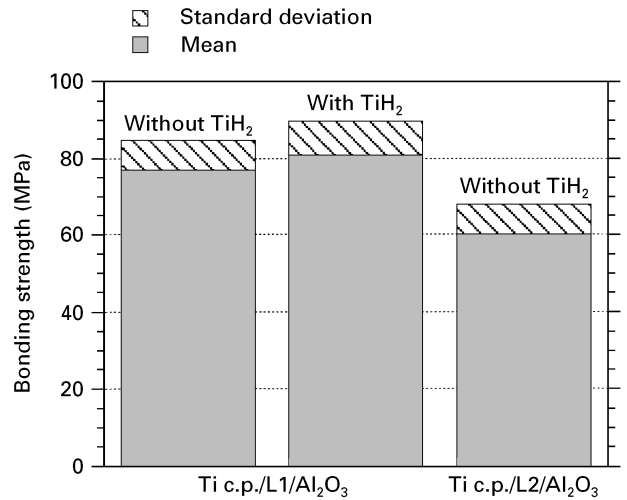


Figure 9 Bonding strength values obtained in the three-point bending tests for the several Ti c.p./brazing alloys/Al₂O₃ joints.

with alloy L1 for Ti/L1 bonds with TiH₂ additions (81 ± 8 MPa). These results may be attributed to the titanium or the Cu_xTi intermetallic compound (formed at the interface with Al₂O₃) which appears to be a barrier to crack propagation.

Independently of the titanium origin, its presence near the alumina will tend to attenuate the differences of thermal expansion coefficient between the alumina and the brazing alloy. The thermal expansion coefficients of titanium and alumina are very similar, being, respectively, 9.8×10^6 and 7.6×10^6 K⁻¹. This fact can generate a positive mechanical effect, as it tends to minimize thermal stresses during the cooling stage.

3.5. Electrochemical characterization of Ti/Al₂O₃ bondings

The electrochemical techniques used to characterize the Ti c.p./Al₂O₃ interfaces were the measurement of the open-circuit potential and potentiodynamic polarizations. Both experiments were performed in a 0.15 M NaCl solution. Table II presents the values obtained for the open circuit potential, E_{corr} , the potential corresponding to current zero, $E(I = 0)$, the Tafel coefficients β_a and β_c , and the polarization resistance, R_p . By introducing the last three values and in the Stern–Geary equation [19] the corrosion current density, i_{corr} , was calculated.

As reported in Table II, the Ti c.p./Al₂O₃ bondings disclose an open-circuit potential, E_{corr} , value lower than Ti c.p. and silver but higher than both brazing alloys L1 and L2. Silver proved to be much more noble than both brazing alloys, as may be seen in Fig. 10. However, the joints produced using silver as bonding agent show a more active behaviour ($E_{\text{corr}} = -269$ mV) than those produced with the alloys L1 and L2 ($E_{\text{corr}} = -123$ and $E_{\text{corr}} = -173$ mV, respectively).

The interpretation of these results is not straightforward. The major elements of the brazing alloys (silver, copper and titanium) behave quite differently in solutions containing chloride ions (Cl⁻). Titanium, being very reactive, tends to auto-passivate when in contact

TABLE II Electrochemical parameters obtained by open-circuit potentials and potentiodynamic polarizations for Ti c.p./Al₂O₃ interfaces. Test solution: 0.15 M NaCl.

Sample references	Open circuit	Potentiodynamic experiments				
	E_{corr} (mV)	$E (I = 0)$ (mV)	β_a (mV)	β_c (mV)	R_p (k Ω cm ²)	i_{corr} (μ A cm ⁻²)
L1	-272	-259	158	380	6.3	7.69
L2	-252	-229	104	320	4.1	8.31
Ag	78	-64	377	221	15.7	3.85
Ti c.p.	68	-297	409	186	738	0.13
Ti/L1/Al ₂ O ₃	-123	-161	100	173	19.9	1.38
Ti/L2/Al ₂ O ₃	-173	-213	348	302	18.7	3.78
Ti/Ag/Al ₂ O ₃	-269	-283	861	215	15.2	4.91

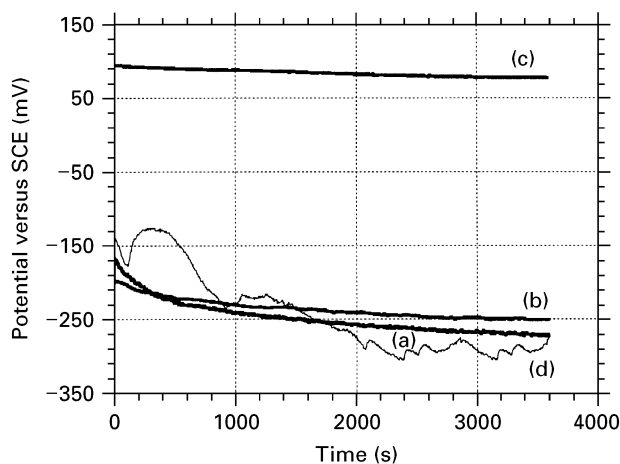


Figure 10 Open-circuit potential measurements: (a) brazing alloy L1, (b) brazing alloy L2, (c) pure silver, (d) Al₂O₃/Ag/Ti c.p. joint.

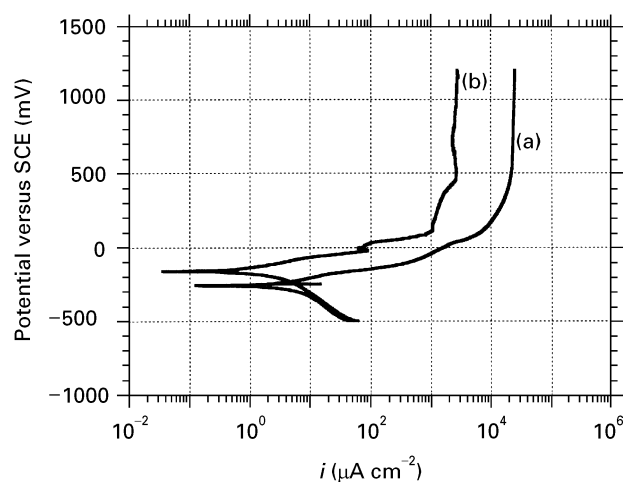


Figure 11 Potentiodynamic polarization curves: (a) L1 brazing alloy and (b) Al₂O₃/L1/Ti c.p. joint.

with air. Subsequently it has a very good resistance to solutions with high concentrations of Cl⁻. It is only possible to nucleate pits for potentials around 2000 mV [20]. Silver is *per se* noble and, furthermore, due to the low K_{ps} of AgCl, tends to passivate in Cl⁻-containing solutions [21]. On the contrary, copper forms soluble complexes (for instance [CuCl₂]) and corrodes actively [21].

It is based on these types of behaviour that the obtained data should be analysed. Alloy L2 (46 wt%) corrodes at a higher rate than alloy L1 (26 wt%), due to its higher amount of copper. For the same reason, and as a consequence of the formed microcathodic and microanodic areas, both alloys disclose a faster corrosion kinetics than silver. Joints produced with alloy L2 degrade faster than those joints produced with alloy L1. The explanation for the higher i_{corr} values obtained systematically for the alloys *per se*, when compared with the correspondingly produced joints, must be related to the (titanium substrate/brazing alloy) relative areas, which is always around 12:1. However, values are much higher than those obtained by weighted averaging, which indicates that some galvanic sinergetic effect occurred.

Fig. 11 plots the polarizations curves for alloy L1 and the Ti/L1/Al₂O₃ joint. We must also state that Ti c.p./Ag/Al₂O₃ brazed joints, quite unexpectedly,

corrode faster than the joints produced with alloys L1 and L2. This behaviour may be explained in the following way. As silver does not tend to form any complex, being passivated and more noble than titanium [22], there is a tendency for the microanodic areas to be localized within the Ti c.p. sheet. This seems to generate the depassivations responsible for the higher corrosion rates determined in the polarization experiments. Fig. 10 presents an $E = f(t)$ curve (d) that confirms this behaviour, as successive potential oscillations are observed during the experimental period. In Fig. 11, potentiodynamic polarization curves for alloy L1 and Ti c.p./L1/Al₂O₃ joints are presented. These cases correspond to the more corrosion-resistant materials of the tested brazing alloys and joints.

3.6. Atomic absorption spectroscopy (AAS)

Table III presents the ion release levels, to the testing solutions after electrochemical tests, as determined by atomic absorption spectroscopy. The titanium and silver levels are below the equipment detection limit and these results, as a consequence, are not conclusive. However, the higher levels of metallic dissolution were detected for copper, in the joints produced with the L2 brazing alloy. That type of joint shows a higher

TABLE III Metal ion release levels detected in the testing solutions after electrochemical experiments. Reported values were obtained by AAS

Sample	Ti (p.p.m.)	Ag (p.p.m.)	Cu (p.p.m.)	Al (p.p.m.)
Ti c.p.	< 1	–	–	–
Ti c.p./L1/Al ₂ O ₃	< 1	< 0.5	0.12	0
Ti c.p./L2/Al ₂ O ₃	< 1	< 0.5	0.19	0
Ti c.p./Ag/Al ₂ O ₃	< 1	< 0.5	–	0

corrosion rate. On the brazed joints produced with alloy L2, a higher ion release of copper to the testing solutions was detected. This is a result of the higher corrosion rates determined for these materials, as has been discussed previously.

4. Conclusion

By using an active brazing technique it was possible to produce Ti c.p./Al₂O₃ joints with good properties. The best results, both in terms of mechanical strength and corrosion resistance of the produced interfaces, were obtained using a Ag–26 Cu–3 Ti brazing alloy. However, in all the cases studied (alloys L1 and L2), the results seem to be quite satisfactory, as most of the fractures occurred within the alumina and not at the brazing alloy. This clearly indicates that the bonds are strong enough with both brazing alloys.

The brazing method tested in this work, on which a TiH₂ layer is spread on the ceramic surface, seems to be a good alternative to the joining techniques currently used. The processing route presented here allows for the substitution of the usual sequence – metallizing, plating and brazing – by a direct brazing in which the pretreatments are replaced by the use of the TiH₂.

Acknowledgements

The support of the BRITE/EURAM programme under project BREU 0323-CT90 is gratefully acknowledged. O. C. Paiva is also grateful to JNICT the award of an MSc scholarship which supported the earlier stages of this research.

References

- O. C. PAIVA and M. A. BARBOSA, in “Advances in Materials Science and Implant Orthopaedic Surgery”, edited by R. Kossowsky and N. Kossowsky (NATO ASI Series, Dordrecht, The Netherlands 1995) p. 275.
- H. HONGQI, J. ZHIIHAO and W. XIAOTIAN, *J. Mater. Sci.* **29** (1994) 5041.
- M. L. SANTELLA, *Ceram. Bull.* **6** (1992) 947.
- M. M. SCHWARTZ, “Ceramic Joining” (ASM International, Ohio, USA, 1990).
- M. NICHOLAS and D. MORTIMER, *Mater. Sci. Technol.* **1** (1985) 657.
- G. P. KELKAR and A. H. CARIM, in “Ceramic Transactions - Structural Ceramics Joining II”, edited by A. J. Moorhead, R. E. Loehman and S. M. Johnson (American Ceramic Society, Ohio, USA, 1993).
- J.-G. LI, *Ceram. Int.* **20** (1994) 391.
- H. MIZUHARA, E. HUEBEL and T. OYAMA, *Ceram. Bull.* **9** (1989) 1591.
- M. D. JACKSON, “Welding Methods and Metallurgy” (Griffin Editions, London, 1966).
- R. E. LOEHMAN and A. P. TOMSIA, *Ceram. Bull.* **2** (1988) 375.
- M. A. BARBOSA, L. ROCHA and P. PURES, in “Monitoring of Orthopedic Implants - A Biomaterials/Microelectronics Challenge”, edited by F. Burny and R. Pures (Elsevier Science, North-Holland, 1993) p. 222.
- R. CASSIDY, R. PENCE and W. MODDEMAN, *Ceram. Eng. Sci. Proc.* **10** (1989) 1582.
- F. BARBIER, C. PEYTOUR and A. REVCOLEVSCHI, *J. Am. Ceram. Soc.* **6** (1990) 1582.
- R. E. LOEHMAN and A. P. TOMSIA, *Acta Metall. Mater.* **40** (1992) S75.
- M. G. NICHOLAS and D. A. MORTIMORE, *Mater. Sci. Technol.* **1** (1985) 657.
- M. G. NICHOLAS Br. *Ceram. Trans. J.* **85** (1986) 144.
- M. G. NICHOLAS and R. M. CRISPIN, *Ceram. Eng. Sci. Proc.* **10** (1989) 1602.
- A. K. MISRA, *Metall. Trans.* **22A** (1991) 715.
- M. STERN and A. L. GEARY, *Corrosion* **13** (1957) 139.
- M. A. BARBOSA, in “Biomaterials - Hard Tissue Repair and Replacement”, edited by D. Muster (Elsevier Science, North-Holland, 1992) p. 257.
- H. H. UHLIG, “Corrosion and corrosion control” (Wiley, New York, 1967).
- L. L. SHREIR, “Metal/Environment Reactions”, Vol. 1 (Newnes-Butterworths, London, 1978).

Received 8 January

and accepted 18 March 1996